https://doi.org/10.2352/ISSN.2470-1173.2017.18.COLOR-056
© 2017, Society for Imaging Science and Technology

A Novel Colour Hessian and its Applications

Saman Tahery , Mark S. Drew
Simon Fraser University
Vancouver, Canada
samant,mark@cs.sfu.ca

Abstract

The idea of contrast at a pixel, including contrast in colour or higher-dimensional image data, has traditionally been associated with the Structure Tensor, also named the di Zenzo matrix or Harris matrix. This 2×2 array encapsulates how colour-channel first-derivatives give rise to change in any spatial direction in x, y. The di Zenzo or Harris matrix Z has been put to use in several different applications. For one, the Spectral Edge method for image fusion uses Z for a putative colour image, along with the Z for higher-dimensional data, to produce an altered RGB image which properly has exactly the same Z as that of high-D data. So e.g. the contrast from RGB + NIR images can be fused such that Z in RGB takes on the same values as Z for 4-D data. As well, Z has been used as the foundation for the Harris interest-point or corner-point detector. However, a competing definition for Z is the 2×2 Hessian matrix, formed from second-derivative values rather than first derivatives. In this paper we develop a novel Z which in the first place utilizes the Harris Z, but then goes on to modify Z by adding some information from the Hessian. Moreover, here we consider an extension to a Hessian for colour or higher-D image data which treats colour channels not as simply to be added, but in a colour formulation that generates the Hessian from a colour vector. For image fusion, experiments are carried out on three datasets of 50 images each. Using the modified version of Z that includes Hessian information, results are shown to retain more details and also generate fused images that have smaller CIELAB errors from the original RGB. Using the new Z in corner-detection, the novel colour Hessian produces interest points that are more accurate, and as well generates fewer mistake points.

Introduction

Interest point detection has uses in many different fields in computer vision, such as patch matching [1], object recognition [2], and others. An interest point usually refers to a *corner* since corners are points that carry a substantial amount of information about different features of an image. Since Moravec's [3] idea of the application of corner and edge detection to obstacle avoidance in 1980, corner detection has been widely used in many different fields. A Harris matrix H [4] is a 2×2 matrix composed of products of the gradients of image pixels in the x and y directions, I_x, I_y, where subscript x and y refer to partial derivatives. For an *RGB* image R, matrix H has two eigenvalues λ_1 and λ_2 which both take on high values in the case of interest points, hence its use in corner detection. Although there are many variant approaches for finding corners, the Harris corner detector still remains one of the most popular corner detectors in computer vision.

On another tack involving the Harris matrix, image fusion, the process of creating a new image from the information in a set of related images [5], is central in converting multi-channel images into images that are understandable on a monitor by humans for use and analysis. Recently, as dimensionality has increased in remote sensing [6] and satellite imaging [7], image fusion has become an increasingly prominent topic of interest. To date there have been several approaches for image fusion, from high pass filtering techniques to uniform rational filter banks and Laplacian pyramids. In the Spectral Edge (SpE) approach [8], the gradient for a representative *RGB* output image is in large measure preserved while exactly preserving colour contrast derived from a higher-dimensional multispectral image dataset. In SpE, a 2×2 structure tensor matrix Z is used (also called the di Zenzo matrix [9]), where Z is identical to a Harris matrix. The Harris matrix encapsulates colour contrast, and SpE makes use of this by remapping colour gradients such that Z is preserved.

A typical use of SpE is in carrying out image fusion for an *RGB* image plus an accompanying, spatially registered, near infrared (*NIR*) image. The Harris matrix is still 2×2 but captures contrast for the entire 4-dimensional collection of image data. In this way, image data information from the *NIR* image informs the multi-dimensional contrast and SpE changes the initial *RGB* so that it includes *NIR* information. Although we get rather good image fusion results in SpE using Harris, here we define a new definition of Z: the novel idea is to modify Z so as to include some content due to a different descriptor of colour contrast, the Hessian matrix.

The paper proceeds as follows: in §2 we define Harris and Hessian corner detectors. In §3 we explain image fusion and a recent method, Spectral Edge, for image fusion. In §4 we introduce our new method and its use in both corner detection and image fusion. Finally in §5 we discuss experiments using the new descriptor.

Harris and Hessian Corner Detection

A good many interest point detectors ([10, 11, 12, 4, 13, 14, 15]) and evaluations of them ([16, 17]) have been studied. Here we focus on Harris and Hessian detectors.

Harris Corner detection

Harris corner detector is an improved version of Moravec's corner detector [3]. The basic idea of Harris corner detection is as follows: considering a pixel in a greyscale image I, if we are in a flat region then shifting the pixel's local region in any direction would not lead to a change in intensity. For a corner, however, a shift should give a large intensity change when moving the square in any direction. Image derivatives arise when we are taking very small shifts: the result of the analysis is that the intensity change

is high when both eigenvalues of the image derivatives matrix H are high. For a greyscale image I, the Harris matrix H is defined as

$$H = \begin{bmatrix} I_x^2 & I_x I_y \\ I_x I_y & I_y^2 \end{bmatrix} \tag{1}$$

Harris and Stephens [4] then define a measure R of corner response (corner "energy") in terms of eigenvalues $\lambda_1, lambda_2$ of matrix H as follows: let

$$R = \lambda_1\lambda_2 - \kappa(\lambda_1+\lambda_2)^2 = det(H) - \kappa \cdot trace^2(H) \tag{2}$$

with κ being a tunable sensitivity parameter which is between 0.04 and 0.06. Note that the definition of R obviates having to actually calculate eigenvalues (although this is merely an analytic calculation for a 2×2 matrix). Corner points are then defined by finding the maximum of R in each region of the image. Here, the derivatives of the matrix are calculated by convolution with the mask $[-2,-1,0,1,2]$ followed by application of a Gaussian smoothing kernel with width σ. We utilize the default value $\kappa =$ 0.04, and obtain a value R for each pixel. Then the corners would be the local maxima of R, found via non-maximum suppression.

In this paper a colour Harris corner detector is defined by simply filtering the image with a Gaussian mask and then combining the derivatives of each colour channel in the x and y directions, ending up with $L_{xR}, L_{yR}, L_{xG}, L_{yG}, L_{xB}, L_{yB}$. Then a colour Harris corner measure is here defined as follows:

$$\begin{aligned} L(x) &= g(\sigma_I) \otimes I(x) \\ L_x^2 &= L_{xR}^2 + L_{xG}^2 + L_{xB}^2 \\ L_y^2 &= L_{yR}^2 + L_{yB}^2 + L_{yB}^2 \\ M_x M_y &= L_{xR}L_{yR} + L_{xG}L_{yG} + L_{xB}L_{yB} \end{aligned} \tag{3}$$

where operator $\otimes$ indicates convolution. We then insert (3) into the Harris corner measure as follows:

$$R = L_x^2 L_y^2 - (M_x M_y)^2 - k(L_x^2 + L_y^2)^2 \tag{4}$$

Note that we did not specifically define a new Harris matrix, but instead simply developed a colour version of the corner energy by analogy to the scalar greyscale image case.

Fig. 1 shows a pseudocolour view of the corner measure R, with highest to lowest values mapped from red to dark blue. Then we generate local maxima via local non-maximum suppression, shown in Fig. 2(a); in Fig. 2(b) the source image is displayed with corner points overlaid in red.

To date, different uses and adaptations of the Harris corner detector have been developed, such as a scale invariant version [18]; motion tracking and 3D structure from motion recovery using the Harris matrix [19]; a so-called quasi-invariant edge and corner detection [20], and so on.

Hessian corner detection

The Hessian matrix is another 2×2 symmetric square matrix, but constructed out of second-order partial derivatives as opposed to the first derivatives in the Harris detector. The Hessian is

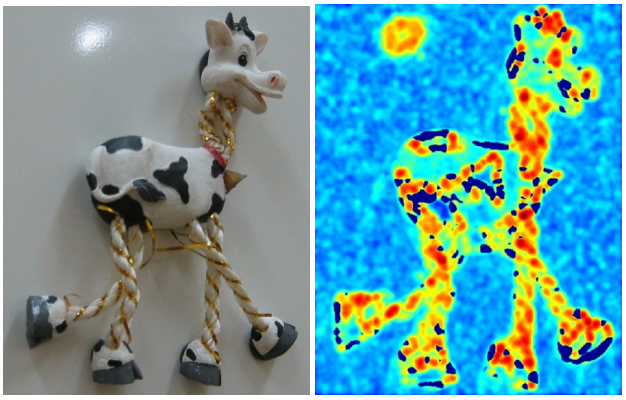

(a) Sample image (b) R mapped to pseudocolour

Figure 1. *Sample image and its corner measure R*

(a) Local maxima (b) Output image with cornerpoints

Figure 2. *maximum points and final corner detection*

an alternative formulation that has been used for corner detection [21]. For a greyscale image I, the Hessian is defined as

$$Hess = \begin{bmatrix} I_{xx} & I_{xy} \\ I_{xy} & I_{yy} \end{bmatrix} \tag{5}$$

Then the feature-point "energy" is defined as the determinant of $Hess$, thus generating a scalar measure of corner-ness:

$$HessEnergy = I_{xx}I_{yy} - (I_{xy})^2 \tag{6}$$

For an RGB image, this has been extended in prior art [22] to a scalar energy

$$HessEnergy = \left[\sum_{k=1}^{3}\left(R_{xx}^k R_{yy}^k - (R_{xy}^k)^2\right)^2\right]^{1/2} \tag{7}$$

where $R^k = (R,G,B)$ for $k = 1..3$.

The algorithm for corner detection using this Hessian-based detector is the same as for the Harris corner detection energy (2) [23, 24] but with the difference that whereas Harris uses first derivatives the Hessian uses second derivatives.

The Hessian matrix has the advantage of capturing local structure for a selected pixel, without canceling the opposing vectors which can happen when we add the first derivatives of each channel. Note that for the Hessian as well, a Gaussian smoothing kernel σ_I^2 is applied to the image, mostly used to remove noise.

One important property of the Hessian to note is that it is actually a re-definition of the Laplacian-of-Gaussian (*LoG*) operator. I.e., what we are doing in forming the *LoG* is first smoothing the image with a Gaussian filter and then taking the Laplacian for each pixel of the image: the Laplacian is

$$\Delta(x,y) = \frac{\partial^2 I}{\partial x^2} + \frac{\partial^2 I}{\partial y^2} \tag{8}$$

which gives us

$$LoG(x,y) = -\frac{1}{\pi\sigma^4}\left[1 - \frac{x^2+y^2}{2\sigma^2}\right] e^{-\frac{x^2+y^2}{2\sigma^2}} \tag{9}$$

which is identical to equation (7).

Novel Colour Hessian

In effect, the extension above of the definition of Hessian corner-ness to colour has been by analogy with that scalar value for greyscale. Instead, here we consider a colour Hessian matrix as a whole. Instead of starting with a 2×2 matrix, we instead develop a 6×2 matrix formed by analogy to the greyscale case, eq. (5), which more naturally takes into account the 3-D nature of colour second-derivatives:

$$Hess = \begin{bmatrix} R_{xx} & R_{xy} \\ G_{xx} & G_{xy} \\ B_{xx} & B_{xy} \\ R_{xy} & R_{yy} \\ G_{xy} & G_{yy} \\ B_{xy} & B_{yy} \end{bmatrix} \tag{10}$$

For this novel definition of a colour Hessian matrix, we can define a colour contrast matrix as

$$Z_{Hess} = Hess^T\, Hess\,, \tag{11}$$

a 2×2 array. The determinant of this matrix gives an energy which is very different from (7).[1] We found that making use of this new quantity improved corner detection, and in the remainder of the paper we exclusively make use of this definition. We also found that adding a quantity of this new matrix Z_{Hess} to the Harris-based colour contrast matrix Z improves colour rendition in the SpE image fusion method.

[1]The determinant is given by the expression $B_{xx}^2 * B_{yy}^2 + B_{xx}^2 * G_{xy}^2 + B_{xx}^2 * G_{yy}^2 + B_{xx}^2 * R_{xy}^2 + B_{xx}^2 * R_{yy}^2 - 2 * B_{xx} * B_{xy}^2 * B_{yy} - 2 * B_{xx} * B_{xy} * G_{xx} * G_{xy} - 2 * B_{xx} * B_{xy} * G_{xy} * G_{yy} - 2 * B_{xx} * B_{xy} * R_{xx} * R_{xy} - 2 * B_{xx} * B_{xy} * R_{xy} * R_{yy} + B_{xy}^4 + B_{xy}^2 * G_{xx}^2 + 2 * B_{xy}^2 * G_{xy}^2 + B_{xy}^2 * G_{yy}^2 + B_{xy}^2 * R_{xx}^2 + 2 * B_{xy}^2 * R_{xy}^2 + B_{xy}^2 * R_{yy}^2 - 2 * B_{xy} * B_{yy} * G_{xx} * G_{xy} - 2 * B_{xy} * B_{yy} * G_{xy} * G_{yy} - 2 * B_{xy} * B_{yy} * R_{xx} * R_{xy} - 2 * B_{xy} * B_{yy} * R_{xy} * R_{yy} + B_{yy}^2 * G_{xx}^2 + B_{yy}^2 * G_{xy}^2 + B_{yy}^2 * R_{xx}^2 + B_{yy}^2 * R_{xy}^2 + G_{xx}^2 * G_{yy}^2 + G_{xx}^2 * R_{xy}^2 + G_{xx}^2 * R_{yy}^2 - 2 * G_{xx} * G_{xy}^2 * G_{yy} - 2 * G_{xx} * G_{xy} * R_{xx} * R_{xy} - 2 * G_{xx} * G_{xy} * R_{xy} * R_{yy} + G_{xy}^4 + G_{xy}^2 * R_{xx}^2 + 2 * G_{xy}^2 * R_{xy}^2 + G_{xy}^2 * R_{yy}^2 - 2 * G_{xy} * G_{yy} * R_{xx} * R_{xy} - 2 * G_{xy} * G_{yy} * R_{xy} * R_{yy} + G_{yy}^2 * R_{xx}^2 + G_{yy}^2 * R_{xy}^2 + R_{xx}^2 * R_{yy}^2 - 2 * R_{xx} * R_{xy}^2 * R_{yy} + R_{xy}^4$.

Image Fusion and SpE

Fusion of multispectral image data is an important current research field: we would like to visualize higher-dimensional image data in a comprehensible way. Having different image data modalities such as NIR, radar, magnetic resonance imaging (MRI), or nuclear magnetic resonance imaging (NMRI) generating a plethora of image pixel data not easily interpretable by human vision, we need to be able to create a high quality output image in a format that can be easily visualized. Image fusion is the process of combining multi-dimensional information, reducing the dimension, whilst keeping the quality of the output image high. It first became a target of interest in 1980 in the field of remote sensing, for hyperspectral data. There are many image fusion methods available (a good summary is [25]). Here we consider the Spectral Edge Image Fusion (SpE) method as enunciated by Connah et al. [8]. This is a gradient-domain approach that maps images of dimension N channels to images of (generally lower) dimension M, with the property of preserving contrast as defined by the structure tensor matrix for the N-D data. The structure tensor matrix was first introduced by di Zenzo [9]. In terms of N-D data C the gradient matrix is defined as follows:

$$\nabla C = \begin{bmatrix} C_x^1 & C_y^1 \\ \vdots & \vdots \\ C_x^N & C_y^N \end{bmatrix} \tag{12}$$

E.g., for RGB data matrix ∇C would have size 3×2. Then the structure tensor Z_C is given by the inner product of ∇C:

$$Z_C = (\nabla C)^T \nabla C \tag{13}$$

Spelled out, this reads

$$Z_C = \begin{pmatrix} \sum_k C_x^k C_x^k & \sum_k C_x^k C_y^k \\ \sum_k C_x^k C_y^k & \sum_k C_y^k C_y^k \end{pmatrix} \tag{14}$$

where k ranges from 1 to N for $N-D$ data. The goal in SpE is to have the same contrast Z_C for both high and low dimensional images. Suppose that we already have a putative RGB image $\tilde{R}$. Then the gradient of $\tilde{R}$ is a 3×2 array $\nabla\tilde{R}$. In SpE, we are looking for a 2×2 transform matrix A from our initial gradient $\nabla\tilde{R}$ to an improved gradient ∇R, such that the new gradient has structure tensor that agrees exactly with that for the high-D gradient ∇C [8]:

$$\nabla R = \nabla\tilde{R}\, A \tag{15}$$

Then insisting on the same structure tensors for high and low dimensional images we have a solution for matrix A as follows:

$$\begin{aligned} & Z_R \equiv Z_C \\ \Rightarrow\quad & Z_R = \nabla R^T \nabla R = A^T \widetilde{\nabla R}^T \widetilde{\nabla R} A \equiv Z_C \\ \Rightarrow\quad & A^T \tilde{Z}_R A \equiv Z_C \\ \Rightarrow\quad & A = (\sqrt{\tilde{Z}_R})^+ \sqrt{Z_C} \end{aligned} \tag{16}$$

Now a problem with using Harris (i.e., the above) as a definition of contrast in SpE is that, although it generates excellent image fusion results, the structure tensor matrix for a 1-channel greyscale image always has only one non-zero eigenvalue. Therefore, in the Harris corner detector, we don't ever use the $det(\cdot)$ part of the Harris energy, just the $trace(\cdot)$ part: i.e., Z has only one non-zero eigenvalue. In Section 4, we introduce a new definition of Z which overcomes this problem and produces improved results.

Adding the Hessian Information

Here, we define a new Z using the novel Hessian matrix Z_{Hess} above (given for example for a 3-D image data in eq.(11)). We add the Hessian-derived contrast matrix Z_{Hess} with a weight factor α^2 to the structure tensor matrix Z_C and denote the resulting combination by ZH. Thus we acquire some of the contrast definition from the Hessian while still having that from the Harris approach persist in influence:

$$ZH \;=\; Z_C + \alpha^2 Z_{Hess} \tag{17}$$

This new ZH turns out to produce better results both in image fusion in terms of maintaining colour plausibility in image fusion images, and in corner detection as well.

Extended Contrast ZH in SpE

Inserting ZH into (16) we have

$$\begin{aligned} & ZR \;\equiv\; ZH \\ \Rightarrow\quad & ZR \;=\; \nabla R^T \nabla R = A^T \widetilde{\nabla R}^T \widetilde{\nabla R} A \;\equiv\; ZH \\ \Rightarrow\quad & A^T \widetilde{ZH}_R \, A \;\equiv\; ZH \\ \Rightarrow\quad & A = (\sqrt{\widetilde{ZH}_R})^{+} \sqrt{ZH} \end{aligned} \tag{18}$$

Thus we can see that the addition of a factor of the Hessian-derived contrast matrix Z_{Hess} to the structure tensor still works for copying higher-D contrast exactly to a lower-D image fusion result, and the transform matrix A is found the same way. In Section 5 we compare the results in terms of colour error from the original *RGB* and see that ZH gives substantially better results than Z alone.

ZH In Corner Detection

In order to use ZH in corner detection, rather than simply using Harris or Hessian matrices alone to calculate a corner measure, we use a matrix ZH given by

$$ZH = \begin{bmatrix} L_x^2 + \alpha^2 L_{xx} & M_x M_y + \alpha^2 L_{xy} \\ M_x M_y + \alpha^2 L_{xy} & L_y^2 + \alpha^2 L_{yy} \end{bmatrix} \tag{19}$$

at each pixel.

Because in corner detection we are usually dealing with an *RGB* image, the novel matrix H will now be

$$H = \begin{bmatrix} R_x & R_y \\ G_x & G_y \\ B_x & B_y \\ \alpha^2 R_{xx} & \alpha^2 R_{xy} \\ \alpha^2 G_{xx} & \alpha^2 G_{xy} \\ \alpha^2 B_{xx} & \alpha^2 B_{xy} \\ \alpha^2 R_{xy} & \alpha^2 R_{yy} \\ \alpha^2 G_{xy} & \alpha^2 G_{yy} \\ \alpha^2 B_{xy} & \alpha^2 B_{yy} \end{bmatrix} \tag{20}$$

This means that the 2×2 array ZH is indeed

$$ZH \;=\; H^T H \;=\; Z_R + \alpha^2 Z_{Hess} \tag{21}$$

so that the corner measure response R_{ZH} becomes

$$R_{ZH} = \sigma_I^2 \; det(ZH) \tag{22}$$

where σ_I is the size of Gaussian kernel we use for our Gaussian filter. We then continue in the same way as previously, finding local maxima and visualizing corners in an output image. In the next section we compare results for corner detection using Harris and ZH and we see that ZH gives better results in detecting corner points.

Experiments and Results

In SpE applied to fusing *RGB* and *NIR*, a 4-dimensional image is constructed to be used in the role of the higher dimensional image, and the desired *RGB* image gradient is just the $A_{2\times 2}$ transform of our *RGB* gradient. Here, for use in our extended cntrast situation, we use the same 4-dimensional $RGB + NIR$ image and compare the CIELAB errors when using Z as compared to using ZH. We carry out experiments by using three different datasets from [26], called "country", "indoor", and "street", each consisting of 50 *RGB* images and corresponding *NIR*. Table 1 shows the CIELAB error for our outputs, compared to the initial We see that using our method significantly reduces colour error.

Figs. 3 and 4 shows sample *RGB* outputs using Z and ZH respectively. We find that the colour looks more natural when using ZH, while for output using Z the colour is quite different from the original image, leading to a loss of image details and substantial CIELAB difference.

In Fig. 5 we compare results for corner detection using the Harris method and our method. We find that corners detected by our method are more accurate and there are no mistakes (detecting a non-corner point). Here tests used $\alpha = 4.0$ and $\sigma = 3.0$.

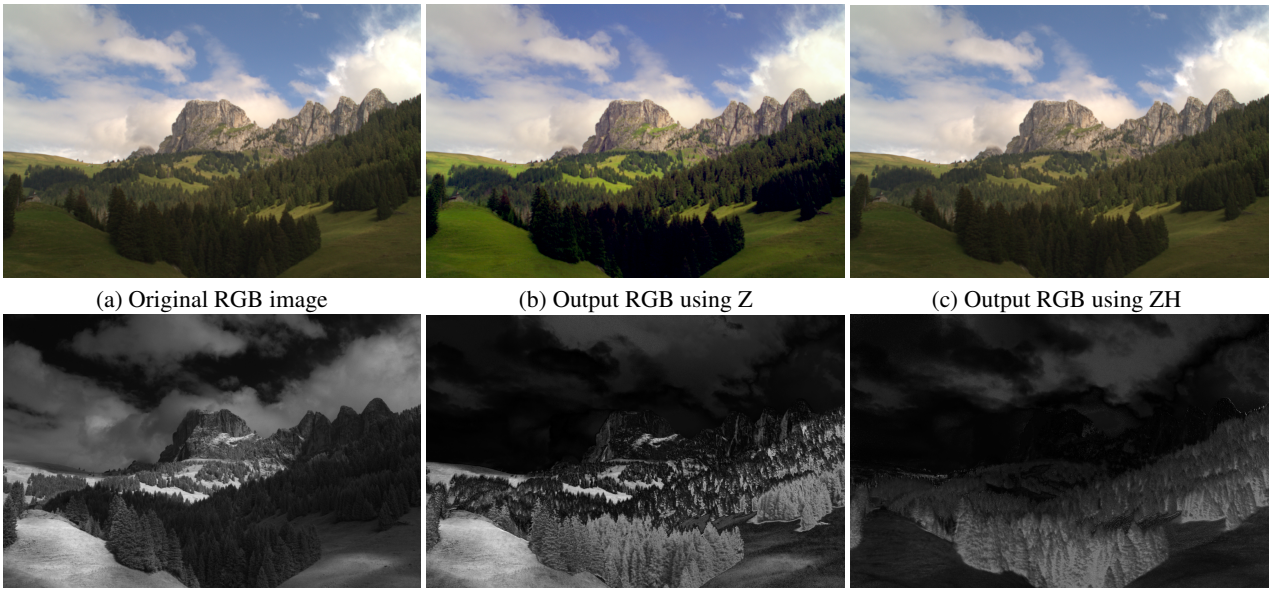

(a) Original RGB image (b) Output RGB using Z (c) Output RGB using ZH

(d) Original NIR image (e) CIELAB Δ_E from original RGB using Z (f) CIELAB Δ_E from original RGB using ZH

Figure 3. *Comparing RGB outputs of SpE using Z and ZH.*

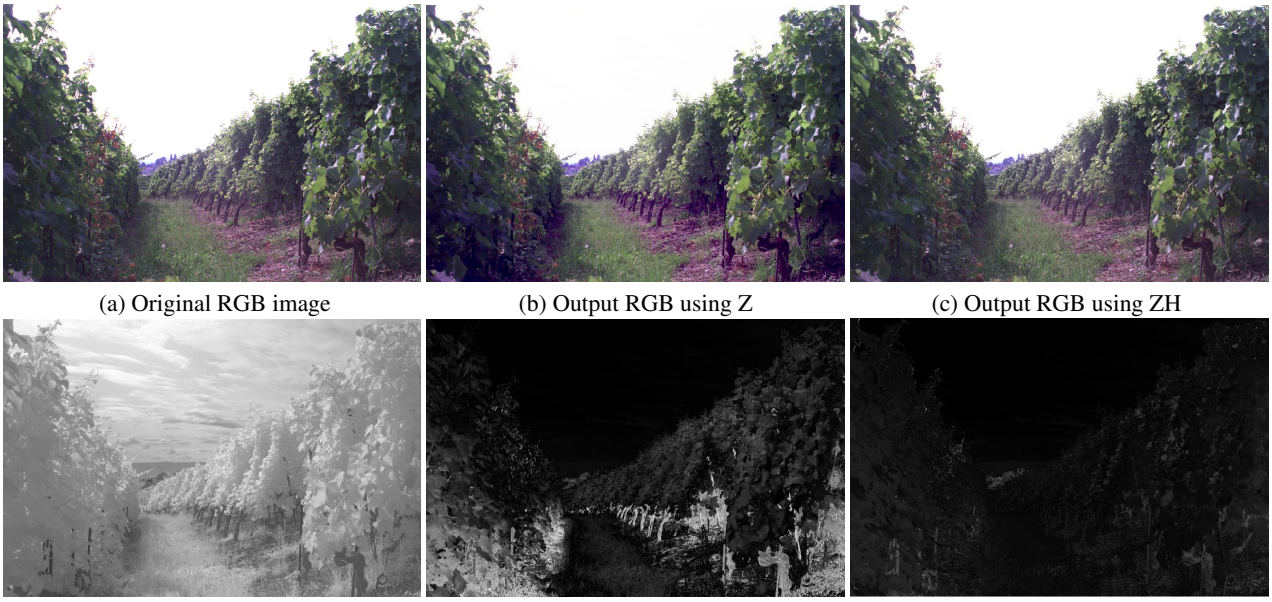

(a) Original RGB image (b) Output RGB using Z (c) Output RGB using ZH

(d) Original NIR image (e) CIELAB Δ_E from original RGB using Z (f) CIELAB Δ_E from original RGB using ZH

Figure 4. *Another example comparing RGB outputs of SpE using Z and ZH.*

Conclusions

Corner detection and image fusion are both topics of current interest that make use of contrast, here colour contrast. In this paper we introduce a new colour contrast descriptor by adding a portion of the Hessian matrix of second derivatives to the Harris matrix of first derivatives. In this way we not only do not lose part of the image information by simply making use of eigenvalues, and moreover also add extra information which improves both the SpE method and Harris corner detection. Our experiments show substantive improvements in both SpE and corner detection, thus justifying the suitability of the new Hessian-based contrast measure. Further research will include using the new *ZH* in other applications.

References

[1] M. Brown, R. Szeliski, and S. Winder, "Multi-image matching using multi-scale oriented patches," in *Comp. Vision and Patt. Rec.*, 2005, pp. 510–517.

[2] G. Csurka, C. R. Dance, L. Fan, J. Willamowski, and C. Bray, "Visual categorization with bags of keypoints," in *In Workshop on Stat.*

Img. Set	Method	CIELAB Err.
Country	Simple Str. Tensor	5.6720
	Extended Str. Tensor	0.0255
Indoor	Simple Str. Tensor	1.3344
	Extended Str. Tensor	0.0387
Street	Simple Str. Tensor	3.1596
	Extended Str. Tensor	0.0287

Table 1: Comparing median CEILAB errors for 3 image sets using SpE with Z (Simple Structure Tensor) and ZH (Extended Structure Tensor), with $\alpha = 5.0$.

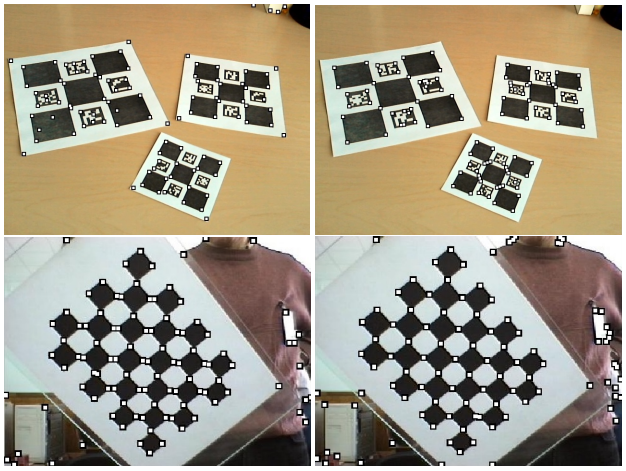

(a) Harris corner detection (b) ZH corner detection

Figure 5. *Detected corners using Harris and ZH method using $\alpha = 4.0$ and $\sigma = 3.0$.*

Learning in Comp. Vis., ECCV, 2004, pp. 1–22.

[3] H. P. Moravec, "Obstacle avoidance and navigation in the real world by a seeing robot rover." DTIC Document, Tech. Rep., 1980.

[4] C. Harris and M. Stephens, "A combined corner and edge detector," in *Alvey Vision Conf.*, 1988, p. 50.

[5] M. B. A. Haghighat, A. Aghagolzadeh, and H. Seyedarabi, "Multi-focus image fusion for visual sensor networks in dct domain," *Computers & Elec. Eng.*, vol. 37, no. 5, pp. 789–797, 2011.

[6] J. B. Campbell and R. H. Wynne, *Introduction to remote sensing*. Guilford Press, 2011.

[7] L. Wald, T. Ranchin, and M. Mangolini, "Fusion of satellite images of different spatial resolutions: assessing the quality of resulting images," *Photogrammetric eng. and remote sensing*, vol. 63, no. 6, pp. 691–699, 1997.

[8] D. Connah, M. S. Drew, and G. D. Finlayson, "Spectral edge: Gradient preserving spectral mapping for image fusion," *J. of the Opt. Soc. of Amer. A,*, vol. 32, no. 12, pp. 2247–2396, 2015.

[9] S. di Zenzo, "A note on the gradient of a multi-image," *Computer vision, graphics, and image proc.*, vol. 33, pp. 116–125, 1986.

[10] J. Matas, O. Chum, M. Urban, and T. Pajdla, "Robust wide-baseline stereo from maximally stable extremal regions," *Image and vis. comput.*, vol. 22, no. 10, pp. 761–767, 2004.

[11] W. Förstner and E. Gülch, "A fast operator for detection and precise location of distinct points, corners and centres of circular features," in *Proc. ISPRS intercommission conf. on fast processing of photogrammetric data*, 1987, pp. 281–305.

[12] S. Smith, "A new class of corner finder," in *British Mach. Vis. Conf.*, 1992, pp. 139–148.

[13] E. Rosten, R. Porter, and T. Drummond, "Faster and better: A machine learning approach to corner detection," *Patt. Anal. and Mach. Intell*, vol. 32, no. 1, pp. 105–119, 2010.

[14] D. G. Lowe, "Distinctive image features from scale-invariant keypoints," *Int. j. of comp. vis.*, vol. 60, no. 2, pp. 91–110, 2004.

[15] C. Tomasi and T. Kanade, *Detection and tracking of point features*. School of Comp. Sci., Carnegie Mellon Univ., Pittsburgh, 1991.

[16] C. Schmid, R. Mohr, and C. Bauckhage, "Evaluation of interest point detectors," *Int. J. of comp. vis.*, vol. 37, no. 2, pp. 151–172, 2000.

[17] A. Gil, O. M. Mozos, M. Ballesta, and O. Reinoso, "A comparative evaluation of interest point detectors and local descriptors for visual slam," *Mach. Vis. and Applications*, vol. 21, no. 6, pp. 905–920, 2010.

[18] D. G. Lowe, "Object recognition from local scale-invariant features," in *Int. conf. on computer vison*, vol. 2, 1999, pp. 1150–1157.

[19] C. Harris, "Geometry from visual motion," in *Active vision*. MIT Press, 1993, pp. 263–284.

[20] J. van de Weijer, T. Gevers, and J.-M. Geusebroek, "Edge and corner detection by photometric quasi-invariants," *Patt. Anal. and Mach. Intell*, vol. 27, no. 4, pp. 625–630, 2005.

[21] S. Krig, *Computer Vision Metrics: Survey, Taxonomy, and Analysis*. Berkeley, CA: Apress, 2014, ch. Interest Point Detector and Feature Descriptor Survey, pp. 217–282.

[22] D. A. Rojas Vigo, F. S. Khan, J. van de Weijer, and T. Gevers, "The impact of color on bag-of-words based object detection," in *Int. Conf. on Patt Rec.*, 2010, pp. 1549–1553.

[23] C. Harris and M. Stephens, "An affine invariant interest point detector," in *European Conf. on Comp. Vis.*, 2002, pp. 128–142.

[24] T. Lindeberg, *Scale-Space*. Wiley Online Library, 2008.

[25] Y. Zhang, "Understanding image fusion," *Photogrammetric eng. and remote sensing*, vol. 70, no. 6, pp. 657–661, 2004.

[26] S. Susstrunk., "RGB-NIR scene dataset." http://ivrlwww.epfl.ch/supplementary_material/cvpr11/, 2011.

Author Biography

Mark S. Drew is a Professor in the School of Computing Science at Simon Fraser University in Vancouver, Canada. His background education is in Engineering Science, Mathematics, and Physics. His interests lie in the fields of image processing, color, computer vision, computer graphics, multimedia, and visualization. He has published over 160 refereed papers and is the holder of 9 patents and applications in computer vision, image processing, and image reconstruction and accenting